



## GROWTH, CHARACTERIZATION AND DOCKING STUDIES OF (2R, 3R)-2-AZANIUMYL-3-HYDROXYBUTANOATE SINGLE CRYSTALS

<sup>1</sup>Maria Claribel Sujatha, <sup>1</sup>J. Satya, <sup>1</sup>C. Vaithyanathan and <sup>2</sup>J. Angel Mary Greena\*

<sup>1</sup>Department of Chemistry, S.T. Hindu College (Affiliated to Manonmaniam Sundaranar University, Abishekapatti, Tirunelveli-12), Nagercoil - 629002, India.

<sup>2</sup>Department of Chemistry, Arignar Anna College, Aralvaimozhi - 629301, India.

\*Corresponding Author: amgreena72@gmail.com

---

### ABSTRACT

Single crystals of (2R,3R)-2-azaniumyl-3-hydroxybutanoate (AA-Z) was grown by controlled slow evaporation method at 5°C. The physico-chemical properties of the grown crystals were understood by single crystal x-ray diffraction (SXR), Fourier transform infrared (FT-IR), UV-Vis spectral and non-linear optical (NLO) studies. SXR confirmed the material of the grown crystal. FT-IR confirms the zwitter ionic nature of the amino acids and supports the SXR structure of AA-Z. UV-Vis spectral studies showed that AA-Z crystals absorb UV radiation and transparent in the visible region. Docking studies with two deadly COVID strains *viz.*, COVID-7N0R and COVID-7R98 was carried out. It was found that ligand AA-Z is two times more effective in binding with COVID-7N0R than with COVID-7R98. The details are reported herein.

**Keywords:** azaniumyl-3-hydroxybutanoate crystals, zwitterionic, docking studies, COVID strains.

---

### 1. INTRODUCTION

Organic crystals attract a great deal of attention due to their wide range of applications in various fields (Ying-Li Shi et al., 2020; Zhiqiang Zhuo et al., 2022; Takenori Tanno et al., 2022). Growth of amino acid crystals has attracted the attention of many researchers because of its specific features like absence of strongly conjugated bonds, hydrogen bonding, molecular chirality, wide transparency ranges in visible and UV spectral regions and zwitter ionic nature (David Madden et al., 2014; Olga Soficheva et al., 2020; Durga Prasad Karothu et al., 2021; Premkumar et al., 2010; Justina et al., 2022). Organic compounds, which possess large pi-electron delocalisation, show good non-linear optical properties. Recently there have been extensive efforts by researchers to grow new amino acid crystals which find excellent applications in non-linear optical field and in optoelectronic devices (Diego Rativa et al., 2010; Ashvin Santhia et al., 2020). The main advantage of working with amino acid crystals is that they allow fine tuning of chemical structures and properties for the desired non-linear optical property (Sooryakala et al., 2021; Davut Avcı et al., 2020). Molecular docking is a useful tool in drug discovery and this has been explored by many researchers in recent years (Luca Pinzi et al., 2019; Azizeh Abdolmaleki et al., 2021). Docking is employed to position small ligands into a receptor structure by simulation. The position of the small ligands in the receptor structure can be modified in a variety of orientations, positions and conformations in

the simulated 3D structure. Docking is found to be very useful in the field of medicine, particularly drug delivery which provides an understanding of the molecular recognition.

In the present study, single crystals of (2R,3R)-2-azaniumyl-3-hydroxybutanoate (AA-Z) were grown by slow evaporation method. The grown crystals were characterised by single crystal XRD, UV-Vis, FT-IR spectral and NLO studies. The potential use of AA-Z as a drug was tested for two COVID strains *viz.*, COVID-7N0R and COVID 7R98 by molecular docking studies.

### GROWTH OF AA-Z SINGLE CRYSTAL

The single crystal of AA-Z is grown by slow evaporation method. 1.16 g of L-threonine was dissolved in 50 ml of ethanol and kept in a beaker tightly closed with perforations in the top so that slow evaporation takes place. The beaker was kept in a cryostat bath and temperature was maintained at 5 °C. Small crystals appeared in the beaker in about a week's time. The grown crystals were harvested after 15 days. The grown AA-Z single crystals were collected, washed with alcohol gently, dried, stored and used for further studies. The maximum size of grown crystals was about 10mm x 2mm x 1 mm. Photograph of the grown AA-Z crystal is shown in figure 1 and the formation of AA-Z single crystal from l-threonine amino acid is schematically shown in figure 2.

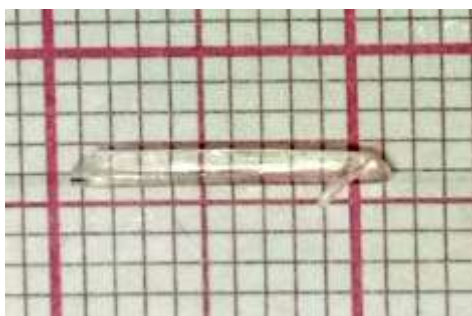


**Figure 1.** Photograph of the grown AA-Z crystal

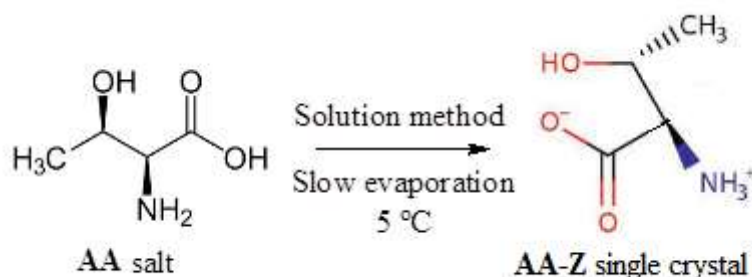


**Figure 2.** Schematic representation of the growth of AA-Z single crystal from AA salt

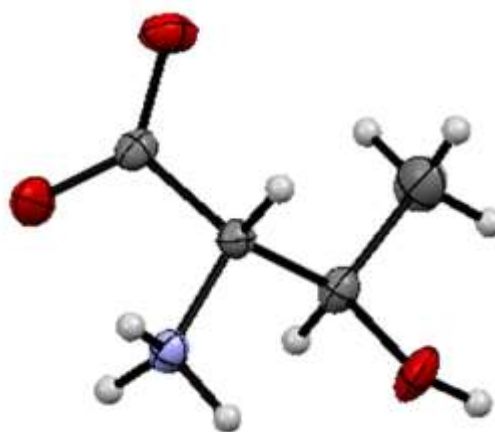
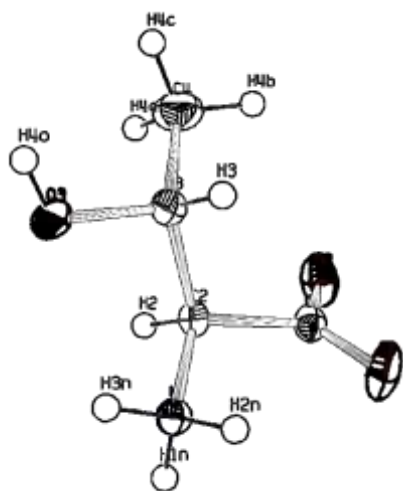
## 2. RESULTS AND DISCUSSION

### 3.1. Single crystal XRD data of AA-Z

The SXRD of AA-Z was recorded in the low angle to the middle angle to get sharp atomic and molecular interactions like covalent bonds, H-bonds and interplanar interactions. Further to fix the lattice points, position of atoms and the bond parameter measurements, the planes were measured precisely by fixing h, k, l indices for wide range. A good agreement was observed in the convergence of independent reflections. A high transition was observed from 96% to 98%. The SXRD data were accepted through F, R, and adjusted  $R^2$  values. Data collected have an accuracy of second decimal point. The extinction coefficient of 110 plane indicates high transparency of the crystal and supports the results. The low root mean square deviation indicates that the values obtained from SXRD are precise. AA-Z has molecular formula  $C_4H_9NO_3$ . Its molecular weight is 119.12, which is agreeable with the calculated molecular formula and weight. This implies that AA-Z has no water of hydration or lattice water. The unit cell is anisotropic in nature with orthogonal axis having no symmetry. The crystal has an orthorhombic geometry, which is the mother of all crystal systems. The crystallographic data of AA-Z and the crystal structure obtained from SXRD is presented in Table 1 and Figure 3 respectively.

**Table 1.** Crystallographic data of AA-Z.

Chemical formula	$C_4H_9NO_3$
Formula weight	119.12 g/mol
Temperature	296(2) K
Wavelength	0.71073 Å
Crystal size	0.150 x 0.220 x 0.280 mm
Crystal habit	clear light colourless Block
Crystal system	orthorhombic
Space group	P 21 21 21
Unit cell dimensions	a = 5.1448(2) Å; $\alpha = 90^\circ$ b = 7.7377(3) Å; $\beta = 90^\circ$ c = 13.6105(6) Å; $\gamma = 90^\circ$
Volume	541.82(4) Å <sup>3</sup>
Z	4
Density (calculated)	1.460 g/cm <sup>3</sup>
Absorption coefficient	0.125 mm <sup>-1</sup>
F(000)	256



O- Red; N-Blue; C-Black; H-White

**Figure 3.**Crystal structure of AA obtained from SXRD**Table 2.** Single crystal structural parameters of AA-Z crystal

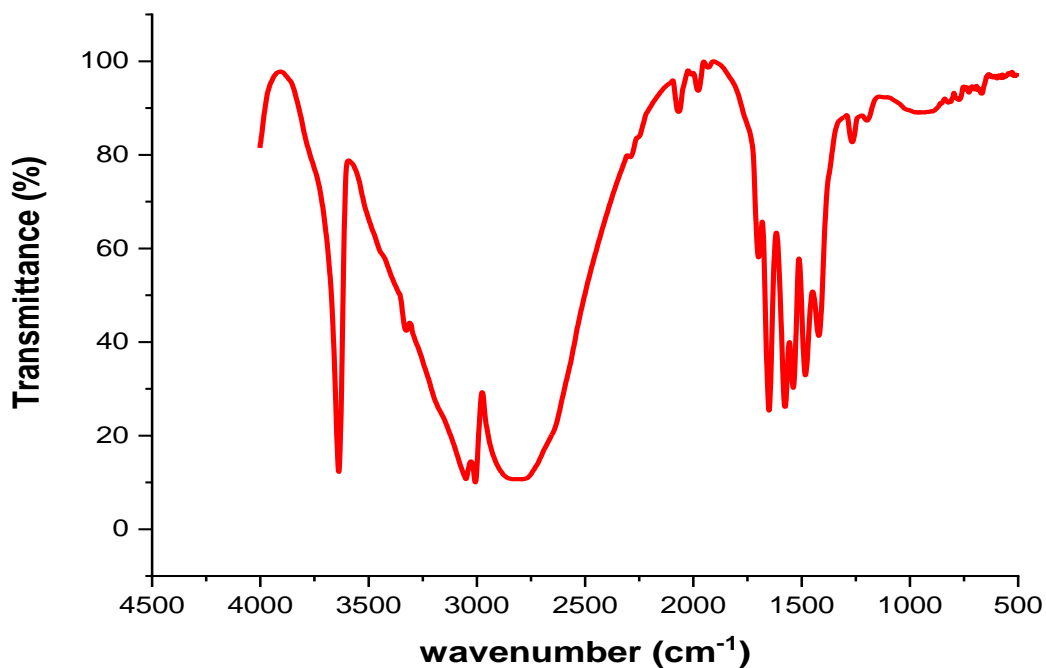
Atom pair	Bond length(Å)	Atom pair	Bond angle (°)
O1-C1	1.241(2)	C2-N1-H1N	109.9(13)
N1-C2	1.489(2)	H1N-N1-H2N	110.0(18)
N1-H2N	0.93(2)	H1N-N1-H3N	107.8(18)
C1-C2	1.535(2)	O1-C1-O2	127.16(16)
O3-H4O	0.80(3)	O2-C1-C2	116.25(14)
C4-H4A	0.96	C3-C4-H4A	109.5
C4-H4C	0.96	H4A-C4-H4B	109.5
C3-H3	0.98	H4A-C4-H4C	109.5
O2-C1	1.249(2)	O3-C3-C4	110.84(13)
N1-H1N	0.88(2)	C4-C3-C2	113.46(14)
N1-H3N	0.93(2)	C4-C3-H3	109.4
O3-C3	1.4243(18)	N1-C2-C3	108.65(12)
C4-C3	1.510(2)	C3-C2-C1	112.75(12)
C4-H4B	0.96	C3-C2-H2	108.5
C3-C2	1.529(2)	C2-N1-H2N	112.7(13)
C2-H2	0.98	C2-N1-H3N	111.8(12)

Table 2 gives the geometrical parameters such as bondlength, bondangle, and dihedralangle of AA-Z. The compound AA-Z is aliphatic and its structure agrees with the molecular formula and molecular weight of the amino acid. Structural parameters indicate that AA-Z has four carbon atoms, the carboxylate carbon is  $sp^2$  hybridised and the other three are  $sp^3$  hybridised. The  $-NH_2$  group is attached to the  $\gamma$ -carbon. The acidic hydrogen of the carboxylic group is involved in the protonation of  $-NH_2$  group, resulting in the zwitter ionic form. The negative charge on carboxylate group is stabilized by sharing between two gem oxygen atoms. This leads to the increase and decrease of bondlengths of the two C-O bonds in carboxylate group through resonance. All the bondlengths and bondangles are comparable with standard values. The alcohol is secondary in nature with the C-O bondlength  $0.12\text{\AA}$  less than the standard value. This may be due to the presence of electron deficient- $NH_3^+$  group and electron withdrawing  $COO^-$  in the vicinal position of the -OH group. The positive and negative inductive effects of  $-CH_3$  and  $-OH$  groups are masked due to the presence of  $-NH_3^+$  group and  $COO^-$  group. The molecule is non-planar with tetrahedral geometry and can act as a bidentate ligand through carboxylate group and nitrogen. The  $-OH$  group can form Hydrogen bond between clusters. Intermolecular interaction can be achieved through carboxylate group, amine group and polar hydroxyl group. Thus AA-Z behaves like a salt under normal conditions and is capable of forming intra and intermolecular hydrogen bonds.

### 3.2. FT-IR Spectra of AA-Z

The FT-IR data of AA-Z is given in Figure 4. A broad and strong band around  $3500-2500\text{cm}^{-1}$  is due to the hydrogen bonding, O-H, N-H, C-H symmetric stretching. Strong band

at  $1565\text{cm}^{-1}$  is due to the  $\text{COO}^-$  ion of the carboxylic as a group. This red shift of C=O group is due to the higher resonance stability. The strong band at  $1320\text{cm}^{-1}$  is for C-O and  $1285\text{cm}^{-1}$  due to C-N. FT-IR confirms the zwitter ionic nature of the amino acids and supports the SXRD structure of AA-Z.



**Figure 4.** FT-IR Spectra of AA-Z.

### 3.3. UV-VIS Spectra of AA-Z

Figure 5 is the UV-VIS spectra of AA-Z. The absorption at 285nm corresponds to  $\pi-\pi^*$  transition. The strong absorption at 200nm is for  $\sigma-\sigma^*$ . The absence of  $n-\pi^*$  transition of Nitrogen is accounted for the formation of ammonium ion and by the formation of zwitter ion due to internal protonation of Nitrogen by carboxylic acid. The high optical gap of 4.35eV explains the stability of AA-Z. All absorptions are in the UV region since AA-Z is a colourless compound.

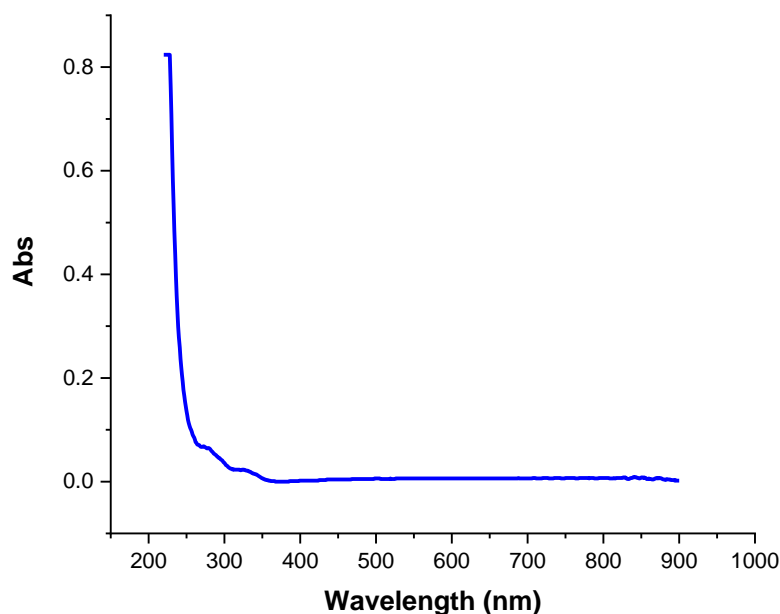


**Figure 5.** UV-VIS Spectra of AA-Z.

### 3.4. Nonlinear Optical Property (NLO) of AA-Z single crystals

Non-linear optics involves the interaction of light and matter. The relation between mass-dielectric polarization vector  $P$  and the incident wave field  $E$  is given as,  $P = \chi E$ , the coefficient  $\chi$  is the electromagnetism of the medium. The optical higher harmonics are derived by  $P = \chi(1)E + \chi(2)EE + \chi(3)EEE + \dots$  where  $\chi(1), \chi(2), \chi(3)$  are the primary, quadratic and cubic polarizability tensors. Results obtained for the NLO activity of AA-Z crystals are given in Table 3 with the field of 0.01 applied through the  $z$ -axis of the molecule. The cubic non-linear polarisation is higher than the quadratic non-linear polarisability.

**Table 3.** Nonlinear optical property of AA-Z.

Components	Axis	Dipole based (au)
Dipole	$z$	2.736
Alpha	$xz$	0.7138
Alpha	$yz$	0.17811
Alpha	$zz$	56.3653
Beta	$xzz$	-52.7321
Beta	$yzz$	2.2913
Beta	$zzz$	-180.44
Gamma	$zzzz$	12964

### 3.5. Molecular Docking Studies of AA-Z

Molecular docking gives information about the interaction between molecules namely drugs, pathogens and proteins in a quantitative manner (Subrakant Jena et al. 2022). The two deadly viral strains chosen for the study are COVID-7N0R and COVID-7R98.

### 3.5.1. Docking of AA-Z with COVID-7NOR

The docking details of AA-Z with COVID-7NOR are given in table 4 and figure 6. Ten binding modes were studied. The first three binding modes were found to be effective. Mode 1 and 2 have synergic interaction between the protein and the AA-Z through threonine and aspartic acid respectively. For mode 1 donor is oxygen and acceptor is hydrogen. For mode 2 both the donor and acceptor atoms are oxygen. The binding through mode 1 is 8.48% higher than mode 2.

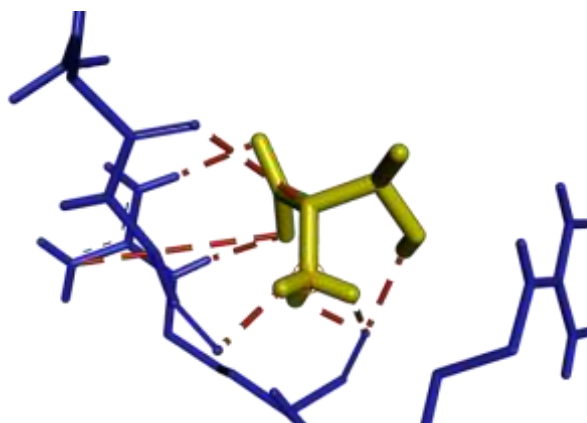


**Figure 6.** Docking of AA-Z with COVID-7NOR.

**Table 4.** Docking of AA-Z with COVID-7NOR.

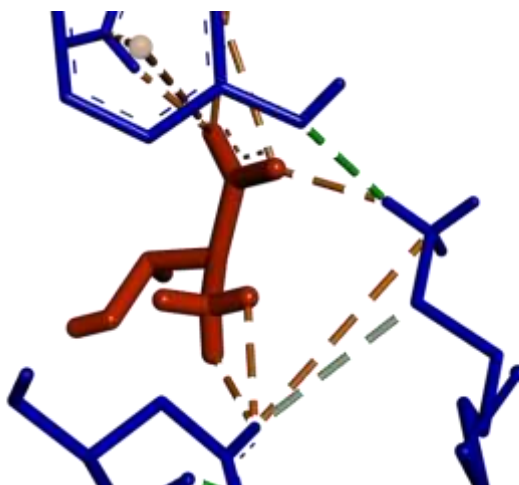
Mode	Binding energy (kcal/mole)	Cluster $r_{msd}$	Reference $r_{msd}$
1	-3.30	0.00	28.21
2	-3.02	0.00	19.01
3	-2.88	0.00	15.91
4	-2.86	0.00	15.03
5	-2.75	0.00	9.24
6	-2.71	0.00	15.86
7	-2.63	0.00	18.79
8	-2.61	0.00	23.72
9	-2.59	0.00	21.81
10	-2.10	0.00	9.59

**Table 5.** Hydrogen bonds

Index	Residue	AA	Distance H-A	Distance D-A	Donor Angle	Protein donor	Side chain	Donor Atom	Acceptor Atom
3	89A	ARG	2.11	3.91	163.5	no	yes	688 [N3]	694 [H]
2	86B	ASP	2.08	4.85	150.58	yes	yes	714 [O3]	726 [O2]
1	128B	THR	1.89	3.45	98.516	yes	yes	4811 [O]	4812 [H]

### 3.5.2. Docking of AA-Z with COVID-7R98

The docking details of AA-Z with COVID-7R98 are given in the table6 and figure 7. Here the binding is through hydrogen bond. Out of ten binding modes, the first three are found to be effective. There is synergic interaction of AA-Z with leucine and glutamic acid side chains. The binding energy of mode 1 is 16.41% higher than that of mode2. For mode2 both donor and acceptor atoms are oxygen. For mode3 the donor is nitrogen and acceptor is oxygen. Thus AA-Z binds COVID-7N0R two times stronger over COVID-7R98.

**Figure 7.** Docking of AA-Z with COVID-7R98.**Table 6.** Docking of AA-Z with COVID-7R98.

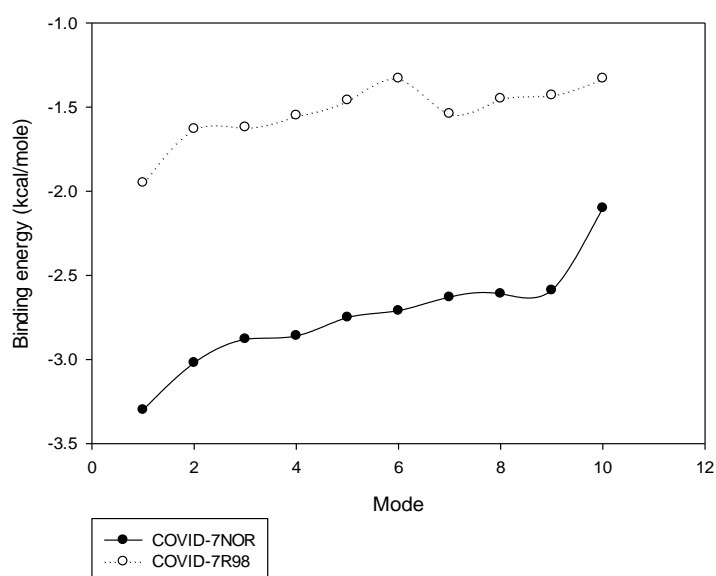
Mode	Binding energy (kJ/mole)	Cluster $r_{msd}$	Reference $r_{msd}$
1	-1.95	0.00	22.41
2	-1.63	0.00	57.58



3	-1.62	0.00	54.40
4	-1.55	0.00	29.93
5	-1.46	0.63	29.72
6	-1.33	1.85	30.07
7	-1.54	0.00	23.59
8	-1.45	0.00	70.26
9	-1.43	0.00	29.96
10	-1.33	0.97	29.49

**Table 7.** Hydrogen bonds

Index	Residue	AA	Distance H-A	Distance D-A	Donor Angle	Protein donor	Side chain	Donor Atom	Acceptor Atom
3	D:ARG19	GLU	3.21	3.06	117.313	yes	no	6989 [N3]	2280 [O3]
2	A:THR1	LEU	2.08	2.22	129.165	yes	yes	6996 [O3]	2163 [O2]

**Figure 8.** Binding energy of AA-Z with COVID-7NOR and COVID-7R98.

### 3. CONCLUSION

AA-Z crystal was successfully grown by slow evaporation method. Crystallographic parameters were determined from SXRD studies. From SXRD studies it was found that the unit cell of AA-Z is anisotropic with orthogonal symmetry. The ionic  $\text{NH}_3^+$  and  $\text{COO}^-$  groups mask the negative and positive inductive effects of  $-\text{OH}$  and  $-\text{CH}_3$  groups. It has intermolecular interaction through the ionic carboxylic acid, amine and hydroxyl group. The positive nitrogen is stabilised by +I and hyper conjugation effects of the hydrogen atoms attached. The crystallisation and zwitter ion formation have no effect on the geometry and has elliptical shape. The carboxylate group is the electron donor and the ammonium ion is the electro acceptor. The hetero atoms in the molecule form external links through hydrogen bonds and columbic interactions and the hydrocarbon part strongly keeps the molecule intact. AA-Z crystals were colourless and absorption were seen only in the UV region. The FT-IR studies proved the presence of the functional groups in the molecule and it is in line with the SXRD data obtained in the present study. The grown crystals were found to be NLO active. Molecular docking studies showed that AA-Z is two times more effective in binding COVID-7N0R than in the case of COVID-7R98. The binding is through hydrogen bonds for COVID-7N0R with threonine and aspartic acid and for COVID-7R98 the binding is with leucine and glutamic acid.

### 4. REFERENCES

- Ashvin Santhia SV, B. Aneeba, S. Vinu, R. et al., L-Threoninum sodium bromide, *Saudi J Biol Sci.*,27: 2987–2992.
- Azizeh Abdolmaleki, Fereshteh Shiri and Jahan B Ghasemi (2021) Use of molecular docking as a decision-making tool in drug delivery, *Molecular Docking for Computer Aided Design: Fundamentals, Techniques, Resources and Applications*, Academic Press, First edition, Chap. 11:229-243
- David C Meddan, Marian L Bentley, Stephen J Jenkins, Stephen M Driver (2014) On the role of molecular chirality in amino acid self-organization on Cu {311}, *Surface Science*, 629:81-87
- Davut Avci, Sümeyye Altrük, Fatih Sönmez, Ömer Tamer, Adil Başoğlu, Yusuf Atalay, Belma Zengin Kurt, Necmi Dege (2020) Synthesis, spectral properties,  $\alpha$ -glucosidase inhibition, second-order and third order NLO parameters and DFT calculations of Cr(III) and V(IV) complexes of 3-methyl picolinic acid, *J. Mol. Struct.*, 1220:
- Diego Rativa, S. J.S. da Silva, J. Del Nero, A. S.L. Gomes, and R. E. de Araujo (2010), Nonlinear optical properties of aromatic amino acids in the femtosecond regime, *J. Opt. Soc. America B* 27:2665-2668
- Durga Prasad Karothu, Ghada Dushaq, Ejaz Ahmed, et al. (2021), Mechanically robust amino acid crystals as fiber-optic transducers and wide bandpass filters for optical communication in the near-infrared, *Nature Communications* 12:1326

- Justina Angelin P., Daniel Sweetlin M., Sumithraj Premkumar P. (2022) Characterization Studies of Solution Grown Triglycine Oxalate Single Crystals, *Crystal Research and Technology* 57 (8), 2100262
- Luca Pinzi and Giulio Rastelli (2019) Molecular Docking: Shifting paradigms in drug delivery, *Int. J. Mol. Sci.*, 20:4331
- Olga S Scficheva, Alina A Nesterova, et al. (2020) The effect of N-substituent on the relative thermodynamic stability of unionised and zwitter ionic forms of  $\alpha$ -diphenyl phosphine- $\alpha$ -aminoacides, *Mendeleev Communications*, 30:516-518
- Premkumar PS, Shajan XS, Devadoss HA. (2010) Optical and thermal studies on pure and doped L-arginine phosphate crystals, *Indian J. Sci. Technol* 3, 253-256
- Sooryakala K, Ramalingam S, Maheswari R, Aarthi R, Venkateswarlu (2021) Electronic controlled optical activity analysis on NLO crystal; 4-amino-5 nitroindole using morphological, spectroscopic and theoretical tools, *Physica B: Condensed Matter*, 604:
- Subrakant Jena, Juhi Dutta, Kiran Devi Tulsian, et al. (2022) Non covalent interactions in proteins and nucleic acids: Beyond hydrogen bonding and  $\pi$  – stacking, *Chem. Soc. Rev.*, 51:4261-4286
- Takenori Tanno, Riyo Shimeda, Takumu Takaya, et al. (2022) Terahertz liner polarizer made of an organic crystal, *Optics & Laser Technol.*, 147:
- Ying-Li Shi, Ming-Peng Zhuo, Xue-Dong Wang and Liang-Sheng Liao (2021) Two Dimensional Organic Semiconductor Crystals for Photonics Applications, *ACS Appl. Nano. Mater.* 3:1080-1097
- Zhiqiang Zhuo, Chuanxin Wei, Mingjian Ni, et al. (2022) Organic molecular crystal with a high ultra deep-blue emission efficiency of  $\approx 85\%$  for low threshold laser, *Dyes and Pigments*, 204: